Molecular Genetics and Metabolism Reports 38 (2024) 101029

Contents lists available at ScienceDirect

Molecular Genetics and Metabolism Reports

journal homepage: www.elsevier.com/locate/ymgmr

In vitro characterization of cells derived from a patient with the *GLA* variant c.376A>G (p.S126G) highlights a non-pathogenic role in Fabry disease

Maximilian Breyer [a], Julia Grüner [a], Alexandra Klein [a], Laura Finke [a], Katharina Klug [a], Markus Sauer [b], Nurcan Üçeyler [a,c,*]

[a] Department of Neurology, University of Würzburg, 97080 Würzburg, Germany
[b] Department of Biophysics and Biotechnology, Biocenter, University of Würzburg, 97074 Würzburg, Germany
[c] Würzburg Fabry Center for Interdisciplinary Therapy (FAZIT), University of Würzburg, 97080 Würzburg, Germany

ARTICLE INFO

Keywords:
Fabry disease
Variants of unknown significance
C.376 A > G (p.S126G)
Globotriaosylceramide
Induced pluripotent stem cells
Sensory neurons
Disease model
α-Galactosidase A

ABSTRACT

Fabry disease (FD) is a life-limiting disorder characterized by intracellular globotriaosylceramide (Gb3) accumulations. The underlying α-galactosidase A (α-GAL A) deficiency is caused by variants in the gene *GLA*. Variants of unknown significance (VUS) are frequently found in *GLA* and challenge clinical management. Here, we investigated a 49-year old man with cryptogenic lacunar cerebral stroke and the chance finding of the VUS S126G, who was sent to our center for diagnosis and initiation of a costly and life-long FD-specific treatment. We combined clinical examination with *in vitro* investigations of dermal fibroblasts (HDF), induced pluripotent stem cells (iPSC), and iPSC-derived sensory neurons. We analyzed α-GAL A activity in iPSC, Gb3 accumulation in all three cell types, and action potential firing in sensory neurons. Neurological examination and small nerve fiber assessment was normal except for reduced distal skin innervation. S126G iPSC showed normal α-GAL A activity compared to controls and no Gb3 deposits were found in all three cell types. Baseline electrophysiological characteristics of S126G neurons showed no difference compared to healthy controls as investigated by patch-clamp recordings. We pioneer multi-level cellular characterization of the VUS S126G using three cell types derived from a patient and provide further evidence for the benign nature of S126G in *GLA*, which is of great importance in the management of such cases in clinical practice.

1. Introduction

Fabry disease (FD) is an X-linked lysosomal storage disorder caused by variants in the α-galactosidase A (α-GAL A) gene (*GLA*) [25]. With an estimated prevalence of 1/8000 [27], FD is the second most common inherited metabolic storage disease [62]. The underlying enzyme malfunction leads to intracellular accumulation of the glycosphingolipid substrate globotriaosylceramide (Gb3) in various organs and tissues. Patients present with diverse symptoms including cardiomyopathy, renal failure, cerebral stroke, and pain due to small fiber neuropathy (SFN) [20]. FD-associated pain is an early hallmark of the disease, with a prevalence of 60–70% in men [21,69]. Traditionally, FD phenotypes were categorized into "classic" with symptom manifestation already in childhood and "late-onset" with milder symptoms starting in adulthood [3,25]. The degree of enzymatic impairment and symptom severity corresponds to the location of the >900 [66] different gene variants known [53] differentiated into "benign" to "pathogenic" [52]. However, some variants remain of unknown significance (VUS). To properly decide on the initiation of FD-specific treatment which is costly, life-long, and may lead to potentially severe side effects [12,28], proper classification of these variants is crucial.

S126G (p.Ser126Gly, c.376 A > G) with a population frequency of 0.06% [11] is such a genetic variant considered "benign" and a VUS [37]. While in one study, end-stage renal disease was described in two patients [72], other studies did not show a pathogenic nature of S126G [15,39,51]. Since previous data was mostly acquired by clinical assessment of patients and enzyme activity measurements [2,15,39], basic science approaches on cellular level, going beyond the established measures, can help to answer the question of pathogenicity and strengthen patients` confidence in medical decisions. Here, we present data on the *GLA* variant S126G, linking thorough clinical examination with a patient-derived *in vitro* system to investigate morphology and

* **Corresponding author at:** Department of Neurology, University of Würzburg, Josef-Schneider-Str. 11, 97080 Würzburg, Germany.
E-mail addresses: breyer_m@ukw.de (M. Breyer), gruener_j@ukw.de (J. Grüner), klein_a6@ukw.de (A. Klein), laura.finke@stud-mail.uni-wuerzburg.de (L. Finke), klug_k1@ukw.de (K. Klug), m.sauer@uni.wuerzburg.de (M. Sauer), ueceyler_n@ukw.de (N. Üçeyler).

https://doi.org/10.1016/j.ymgmr.2023.101029
Received 5 November 2023; Received in revised form 17 November 2023; Accepted 20 November 2023
Available online 25 November 2023

functionality of skin cells, induced pluripotent stem cells (iPSC), and sensory neurons. By analyzing α-GAL A activity, Gb3 accumulation, and neuronal action potential firing, we tested the hypothesis that no molecular signs of FD are found in S126G cells.

2. Materials and methods

2.1. Clinical setting

The 49-year old man was seen at our Fabry Center for Interdisciplinary Therapy Würzburg (FAZIT). One year ago, he had experienced an episode of sensory impairment at the right hand together with an episodic reduction of fine motor skills lasting for few minutes. He also reported acute numbness at the right knee and tingling of the right face. Diagnostic work-up at the Neurological Department in his hometown revealed a punctual lacunar restriction on diffusion-weighted magnetic resonance imaging (MRI) of the brain in the left cerebral hemisphere. Since cardiovascular examinations were normal and the etiology remained obscure, FD diagnostics was initiated in the young patient, which revealed the genetic variant S126G in the *GLA* gene as a chance finding. In the following days, all symptoms resolved completely and the patient reported well-being. No such symptoms had occurred before and since then. Explicit interview also revealed that the patient had never experienced other symptoms characteristic for FD such as acral or other physical pain, hypohidrosis or hearing problems, and did not have angiokeratomas. α-GAL A activity in peripheral blood leukocytes (0.6 nmol/min/mg protein, normal range 0.4–1.0) and lyso-Gb3 (0.6 ng/ml, normal range < 0.9) levels were both normal. Also, family history was negative.

2.2. Clinical examination

The patient underwent complete neurological examination, nerve conduction studies of the right sural and tibial nerves, and a sympathetic skin response test. Further, the somatosensory evoked potentials were recorded upon stimulation of the tibial nerve. For cerebral blood flow, extra- and transcranial duplex sonography was performed and the patient underwent cranial MRI including time-of-flight sequences. For the assessment of small caliber nerve fibers, quantitative sensory testing (QST) was done at the right dorsal foot and a 6-mm skin punch biopsy was taken from the lower leg and the back paraspinally at dermatome level th5 for analysis of intraepidermal nerve fiber density (IENFD). The patient further underwent renal and cardiac assessment to detect potential nephropathy or cardiomyopathy. He had also undergone ophthalmological examination as an outpatient in his home town two years before and provided the medical report.

2.3. Skin biopsy and fibroblast cultivation

Human dermal fibroblasts (HDF) were obtained from the diagnostic skin punch biopsies following a published protocol [68]. For *in vitro* experiments, half of the skin biopsy from the lower leg was used. After mechanical separation of dermis and epidermis, dermal tissue was cultivated in fibroblast expansion medium (Dulbecco's modified eagle's medium/Nutrient Mixture F-12 (Thermo Fisher Scientific, Waltham, MA, USA), 10% fetal calf serum (FCS, Biochrom, Berlin, Germany), 100 U/ml penicillin/streptomycin (Pen/Strep, Thermo Fisher Scientific, Waltham, MA, USA)) under 5% CO_2 and 37 °C [34].

2.4. Generation and cultivation of iPSC

HDF obtained by skin punch biopsy were reprogrammed to iPSC with the StemRNA 3rd Gen Reprogramming Kit (ReproCell, Yokohama, Japan) as previously described [8]. In brief, non-modified RNA coding for reprogramming factors and immune evasion factors, and the microRNA cluster 302/367 were transiently transfected into HDF for four consecutive days using Lipofectamine™ RNAiMAX transfection reagent (Thermo Fisher Scientific, Waltham, MA, USA). Emerging iPSC colonies were isolated and expanded in StemMACS™ iPS-Brew XF, human medium (Miltenyi Biotec, Bergisch Gladbach, Germany) supplemented with 100 U/ml Pen/Strep on hESC qualified Matrigel- (Corning, Corning, NY, USA) coated 6-well plates (Greiner Bio-One, Kremsmünster, Austria) under 5% CO_2 and 37 °C. Routine culture required daily medium change and passaging twice a week using 2 mM EDTA (Thermo Fisher Scientific, Waltham, MA, USA) in phosphate-buffered saline (PBS, Sigma-Aldrich, St. Louis, MS, USA) for detaching. To inhibit apoptosis, 10 μM Y27632 (Miltenyi Biotec, Bergisch Gladbach, Germany) was added to the medium for the first 24 h after passaging. Expanded clones were analyzed for pluripotency factor expression, three-germ-layer-formation potential, normal karyotype, and *GLA* sequence ([8] and Fig. S1).

2.5. Sensory neuron differentiation

iPSC were differentiated to sensory neurons as previously described [36]. In brief, iPSC were seeded into growth factor-reduced Matrigel-coated (Corning, Corning, NY, USA) 6-well plates, cultured until confluence, and differentiated in a ten day protocol with daily change of defined differentiation medium. Until day two, neuralization of iPSC was induced *via* dual SMAD inhibition using the small-molecule inhibitors LDN-193189 and SB431542. Between day three and ten, three additional small-molecule inhibitors (CHIR99021, SU5402, DAPT) acting on WNT-, notch-receptor, and FGF-receptor signaling were applied to obtain nociceptive sensory like neurons *via* a neural crest cell intermediate. From day eleven on, cells were matured for at least five weeks with the addition of β-nerve growth factor (β-NGF), brain-derived neurotrophic factor (BDNF), and glia cell-derived neurotrophic factor (GDNF) to produce fully active post-mitotic sensory neurons.

2.6. Immunocytochemistry

For immunocytochemistry (ICC), iPSC and HDF were seeded on Matrigel- (Corning, Corning, NY, USA) or Cultrex-coated (Bio-Techne, Minneapolis, MN, USA) high-precision glass coverslips (Hartenstein, Würzburg, Germany) two days prior to immunoreaction and pre-seeded sensory neurons were stained five to seven weeks after differentiation. Cells were fixed with 4% paraformaldehyde (Electron Microscopy Sciences, Hatfield, PA, USA) in PBS for 15 min at room temperature, washed with PBS, and unspecific binding was blocked with 5% fetal bovine serum (FBS, Merck, Darmstadt, Germany) in PBS. Primary antibodies were diluted in blocking solution, supplemented with 0.1% saponin for permeabilization, and incubated at 4 °C overnight. Primary antibodies included anti-peripherin (mouse anti-human IgG, conjugated to Alexa Fluor 488, 1:200, sc-377,093, Santa Cruz Biotechnology, Dallas, TX, USA) and anti-vimentin (rabbit anti-human IgG, 1:200, ab92547, Abcam, Cambridge, UK). Cells were washed with PBS and incubated with secondary antibodies diluted in PBS for two hours at room temperature. Secondary antibody used was 488-labeled donkey anti-rabbit IgG (1:100, Jackson ImmunoResearch Europe, Ely, UK). After washing with PBS, coverslips were mounted using Aqua-Poly/Mount mounting solution (Polysciences, Warrington, PA, USA). To label nuclei, 4′,6-diamidino-2-phenylindole (DAPI) was included in the first washing step before mounting. For visualization of intracellular Gb3, Shiga toxin subunit B (STxB, Sigma-Aldrich, St. Louis, MO, USA) was coupled to Alexa Fluor 555 dye (Thermo Fisher Scientific, Waltham, MA, USA) (STxB::555) as previously described [61], and added to the primary antibody solution. Images were acquired on a Zeiss Axio Imager 2 upright microscope (Zeiss, Oberkochen, Germany) controlled by ZEN (blue edition) software (Zeiss, Oberkochen, Germany) and processed with the Fiji distribution of ImageJ software [60].

2.7. α-GAL A activity assay

α-GAL A activity was measured in iPSC with the Alpha Galactosidase Activity Assay Kit (Abcam, Cambridge, UK). In brief, iPSC were lysed *via* ultrasonic pulses, centrifuged, and supernatant containing α-GAL A was collected for analysis. Substrate cleavage by α-GAL A was detected fluorometrically after two hours of incubation at 37 °C using a Tecan microplate reader (Tecan, Männedorf, Switzerland). For normalization, total protein concentration was determined using a BCA assay (Interchim, Montluçon, France).

2.8. Patch-clamp recordings

For electrophysiological recordings, sensory neurons were seeded on Matrigel- (Corning, Corning, NY, USA) or Cultrex-coated (Bio-Techne, Minneapolis, MN, USA) high-precision glass coverslips directly after differentiation and measured after five to ten weeks of maturation. On the day of analysis, neurons were transferred to a microscope chamber filled with physiological bath solution (180 mM NaCl, 5.4 mM KCl, 1.8 mM $CaCl_2$, 1 mM $MgCl_2$, 10 mM glucose, 5 mM HEPES). To form the recording electrode, borosilicate capillaries (Kimble Chase Life Science and Research Products, Meiningen, Germany) were pulled with a P-1000 micropipette puller (Sutter Instrument, Novato, CA, USA) to a final input resistance of 3–6 MΩ, filled with intracellular pipette solution (170 mM KCl, 2 mM $MgCl_2$, 1 mM EGTA, 1 mM ATP, and 5 mM HEPES), and imposed on an Ag/AgCl electrode. A second Ag/AgCl reference grounding electrode was applied to the bath solution directly to close the electrical circuit. Both electrodes were connected to an EPC10 amplifier (HEKA, Ludwigshafen, Germany) controlled by the Patchmaster software (HEKA, Lambrecht, Germany) to inject and measure currents with a sample rate of 20 kHz. Neuronal somas were approached with the recording electrode using a micromanipulator (Luigs & Neumann, Ratingen, Germany). After gigaseal formation, fast pipette capacitance was compensated. Whole-cell (WC) configuration was achieved *via* short suction rupturing the membrane followed by slow membrane capacitance compensation. Electrical configurations and parameters were constantly assessed in Patchmaster *via* a 5-mV test pulse. To control for access integrity during WC configuration, measurements were filtered to an access resistance below 15 MΩ.

To record action potentials (AP), square-wave currents between 0 and 290 pA were injected into the neurons incrementally in 10-pA steps, and the first evoked AP was used to determine AP parameters with Stimfit software [29]. AP amplitude was considered the difference between resting membrane potential and peak depolarized potential, and AP duration was determined at half-maximum amplitude. The threshold potential was determined at the turning point of the AP depolarizing phase characterized by a slope of 5 mV/ms [14]. The minimum current needed to elicit an AP was considered the rheobase of the cell. To investigate firing behavior, APs were counted over 500 ms of stimulation with currents resembling 1×, 2×, 3×, and 4× multiples of the rheobase. Neurons that elicited multiple action potentials were included as nociceptors.

2.9. Statistics

Statistical analysis was performed with SPSS software version 28.0.1.0 (IBM, Ehningen, Germany). Data was analyzed for normal distribution using Shapiro-Wilk test. Normally distributed data were investigated using the Student's *t*-test and one-way ANOVA for two and more than two groups, respectively. Otherwise the nonparametric Mann-Whitney-*U* test was applied. Differences were considered significant at $p < 0.05$ (*p < 0.05, **$p < 0.01$, ***$p < 0.001$). Graphs were generated in Graphpad PRISM software version 9.3.1 (GraphPad Software, Inc., La Jolla, CA, USA).

3. Results

3.1. Normal clinical assessment

Neurological examination was completely normal. Nerve conduction studies of the right sural and tibial nerves showed normal results. Sympathetic skin response at the feet after stimulation at the hand was present and the P40-latencies of the somatosensory evoked potentials were in the normal range. Extra- and transcranial duplex sonography showed normal blood flow. Cranial MRI including time-of-flight sequences was also unremarkable, particularly without white matter lesions or vascular ectasia. QST at the right foot revealed normal mechanic and thermal perception and pain thresholds compared with published normative data [43]. IENFD was reduced at the lower leg (2.1 fibers/mm), while the proximal skin innervation was normal (17 fibers/mm) compared with our laboratory normative values (lower leg: 9 +/-3 fibers/mm; back: 25 +/-8 fibers/mm). Further clinical examination revealed normal renal function with a glomerular filtration rate (e-GFR) of 103 ml/min /1.73 m^2 and no proteinuria. Cardiac function was also normal without cardiomyopathy. Also, no cornea verticillata had been found during an ophthalmological assessment as documented in the respective medical report the patient provided.

3.2. S126G iPSC show normal α-GAL A activity

To assess the effect of the genetic variant S126G on enzyme stability, we first determined the location of serine at position 126 within the α-GAL A homodimer (Fig. 1A). The affected serine resides on the protein surface distant to the active site of α-GAL A. Further, we measured α-GAL A activity in cell lysates of S126G and healthy control iPSC. α-GAL A activity was similar in both genotypes (Fig. 1B).

3.3. No Gb3 deposits are detectable in S126G cells

To test for FD-specific intracellular Gb3 accumulations in S126G cells, fluorescently labeled STxB was used to visualize Gb3 in HDF, iPSC, and differentiated sensory neurons. As a positive control for STxB immunoreaction, we used HDF of a patient carrying the FD-related nonsense variant Q357X. While massive Gb3 deposits were visible in the positive control HDF (Fig. 2A), S126G HDF showed hardly any STxB signal similar to healthy control cells (Fig. 2B). The same was true for iPSC (Fig. 2C) and sensory neurons (Fig. 2D).

3.4. AP firing of S126G sensory neurons equals control cells

To investigate effects of the genetic variant S126G on sensory neuron excitability, AP of iPSC-derived S126G and healthy control neurons were analyzed in current-clamp mode. Fig. 3A shows a representative AP recorded from a S126G neuron with illustration of analyzed parameters. Fig. 3B shows representative AP trains in control and S126G neurons elicited by current injection demonstrating the ability of repetitive firing in sensory neurons of both genotypes.

First, we investigated the shape of the AP characterized by amplitude and duration measured at half maximum width. We found no difference in AP amplitude and duration ($H_{Max\ width}$) between S126G and control neurons, confirming normal shape of the AP in S126G neurons (Fig. 4A, B). In addition, the threshold potential, directly reflecting excitability of neurons [18], showed no difference between S126G and control neurons (Fig. 4C) while the same was true for the resting membrane potential (Fig. 4D). The minimum current needed to elicit an AP (rheobase) showed no difference between S126G and control neurons (Fig. 4E). To further assess neuronal excitability, AP were counted within 500 ms upon stimulation with multiples of the rheobase. While AP firing was lower in S126G neurons for an injected current reflecting 2× the rheobase (Fig. 4F, $p < 0.05$), we found no differences in AP firing between S126G and control neurons for injected currents reflecting 1×, 3×, and

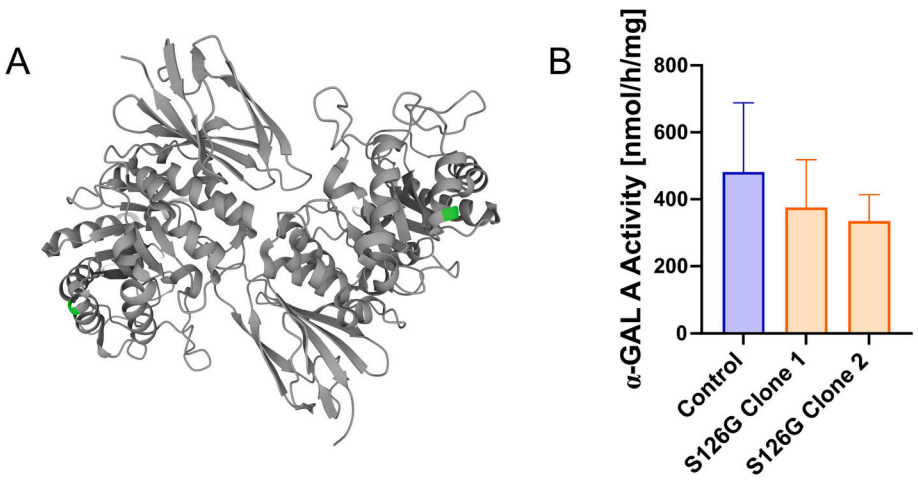

Fig. 1. Variant site and α-GAL A activity in iPSC.
(A) Visualization of α-GAL A homodimer (grey, PDB identifier: 1R46, [24]) including the site affected by the genetic variant S126G (green) on the protein surface. (B) α-GAL A activity measured in cell lysates of a healthy control iPSC clone and two independent S126G clones. No difference in enzyme activity was found for control and S126G iPSC (one-way ANOVA, $n_{Control} = 3$, $n_{S126G} = 3$). Bar graph of means with standard deviations. Abbreviations: α-GAL A, α-galactosidase A; iPSC, induced pluripotent stem cells; PDB, protein data base.

4× the rheobase (Fig. 4F). Overall, no relevant pathological differences in AP shape and firing were found in S126G neurons compared to healthy control neurons.

4. Discussion

FD is a life-threatening disease that requires permanent and costly treatment. Hence, correct diagnosis is critical to protect patients who carry genetic variants without relevant pathogenicity from potential adverse events, but also to determine patients in need of early FD-specific treatment by enzyme replacement [26] or chaperone therapy [74]. Besides infusion-associated symptoms such as fever [63], severe side effects including throat tightness [47], anaphylactic reaction [4,67], and atrial fibrillation [5] were reported.

VUS are a crucial challenge in the clinical management of patients with suspected FD and data available in literature as well as classification in databases is conflicting. Several genetic VUS are known in the *GLA* gene and are controversially discussed such as A143T and D313Y. While some studies report on cardiac involvement and reduced *GLA* activity in A143T [13,70], others did not observe FD-related organ involvement [57,64]. Similarly, D313Y was considered pathogenic due to reports of neurological and renal symptoms [16,76], while no organ manifestation was found in other studies [30,48]. As a result, classification of VUS in databases changes frequently and caregivers have to decide on FD-specific treatment based on the individual case. For S126G, data availability is even more limited. We report on a man who suffered from lacunar cerebral stroke and was diagnosed with FD based on the mere chance finding of the VUS S126G in the *GLA* gene. We have combined neurological examination with the study of patient-derived cells *in vitro* and provide multilevel evidence for a non-pathogenic status of S126G in this patient.

At our center, we diagnosed our patient not to have FD and no FD-specific treatment was recommended. He was instructed to get in touch if any symptoms suspicious of FD occur, which did not happen until the date of this report (*i.e.* in the last four years). In synopsis of all findings, we assume the lacunar cerebral stroke in our patient as etiologically cryptogenic, which is the case in 26% of all stroke patients [50]. *Vice versa*, screening studies for FD in young patients with cerebral stroke of unknown etiology reported a prevalence <1% based on α-GAL A activity and/or genetic testing [1,38,58]. However, considering VUS in such screening approaches can artificially inflate the prevalence up to 7% [17]. The finding of a *GLA* VUS in absence of FD-specific signs and symptoms, negative family history, normal lyso-Gb3, and α-GAL A activity should hence be interpreted with great caution. Particularly the latter is currently considered to exclude FD in a male person per definition.

The effect of a genetic variant on α-GAL A activity is determined by its impact on either integrity of the active site or overall conformational stability [23]. As shown by recent studies, variants residing aside from the active site and α-GAL A core are less prone to cause severe FD symptoms [53,54]. The location of serine 126 on the surface of the enzyme therefore suggests a non-pathogenic variant. In addition, we confirm in iPSC that S126G has no effect on α-GAL A activity (Fig. 1B) as was also reported before [6,49,59]. Assessing enzyme activity *in vitro* was considered the most accurate predictor of FD phenotype compared to plasma lyso-Gb3 and computational algorithms [42]. In contrast to α-GAL A measurement in plasma, cell-based activity assays are further insensitive to false detection of enzymatic pseudodeficiency [7,31]. However, a recent study suggested an impact of the S126G variant on enzyme trafficking towards lysosomes despite normal enzyme activity, questioning the significance of mere α-GAL A activity measurement for FD diagnosis [56]. Further investigation on both substrate and cellular function level was hence advised.

Gb3 is present in many tissues [10], however, investigating deposits in one cell type alone is not sufficient to assess the outcome of a variant. Although α-GAL A activity is determined by the variants position, translation to intracellular Gb3 deposits is likewise dependent on cell type-specific heterogeneous Gb3 metabolism. For instance, it was shown that plasma membrane expression of the receptor Gb3 is regulated by the cell cycle leading to expression differences between proliferative and non-proliferative cells and cell types [44]. We show the corresponding absence of Gb3 accumulation in HDF, epigenetically rejuvenated iPSC, and terminally differentiated sensory neurons (Fig. 2). In FD patient–derived HDF and sensory neurons, massive deposits were previously reported [32,36]. Further, genetic knockout of *GLA* caused intracellular accumulation in otherwise healthy iPSC [33]. Missing detection of STxB signal in all three cell types reinforces the notion of a non-pathogenic role of S126G.

Determination of IENFD with low inter- and intra-observer variability [65] is frequently used in patients with suspected small fiber neuropathy [35,40], however, reduction of skin innervation as a typical finding is not specific [19,71]. Given the reduced distal IENFD in our patient, we analyzed the *in vitro* excitability of sensory neurons carrying the S126G variant. We not only aimed to uncover potential

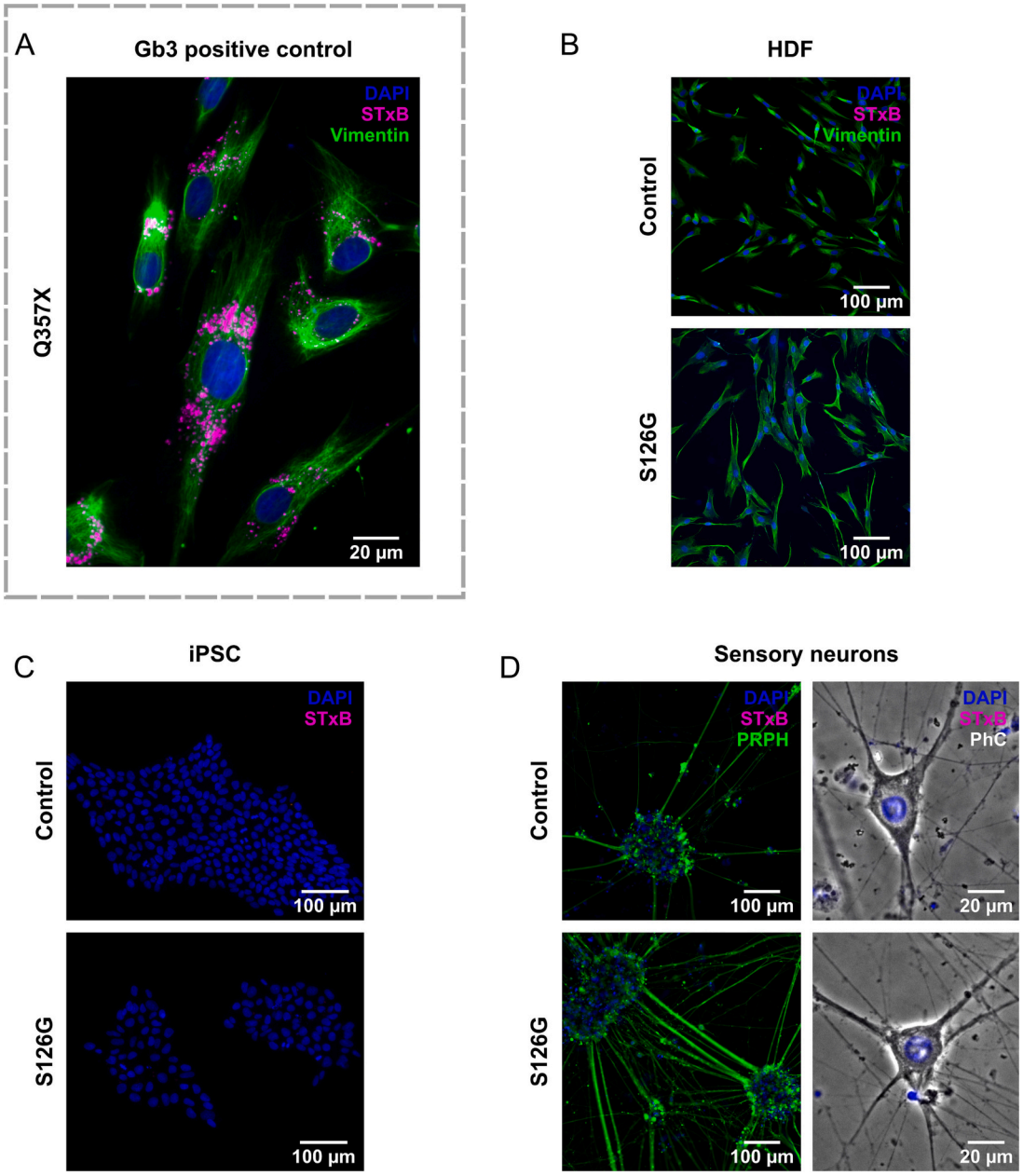

Fig. 2. Visualization of intracellular Gb3 accumulations in healthy control and S126G cells.
(A) Representative photomicrograph of HDF carrying the variant Q357X (nonsense) in the *GLA* gene as positive control for STxB immunoreactivity. Q357X HDF showed massive intracellular STxB::555 signal corresponding to Gb3 deposits. (B) Representative photomicrographs of healthy control and S126G HDF immunoreacted with STxB::555. No Gb3 accumulations were detected in control and S126G HDF. (C) Representative photomicrographs of healthy control and S126G iPSC immunoreacted with STxB::555. No Gb3 accumulations were present in control and S126G iPSC. (D, left) Representative photomicrographs of control and S126G sensory neuron clusters immunoreacted with STxB::555 and the peripheral nervous system marker PRPH. No Gb3 accumulations were found in control and S126G sensory neuron clusters. (D, right) Representative photomicrographs of control and S126G single sensory neuron somas immunoreacted with STxB::555. No Gb3 accumulations were detected in control and S126G sensory neuron somas. Photomicrographs show overlay of fluorescence signal and phase contrast image. Abbreviations: DAPI, 4′,6-diamidino-2-phenylindole; Gb3, globotriaosylceramide; *GLA*, α-galactosidase A gene; HDF, human dermal fibroblasts; iPSC, induced pluripotent stem cells; PhC, phase contrast microscopy; PRPH, peripherin; STxB, Shiga toxin subunit B.

abnormalities reflecting current nerve pathology, but also to predict neuronal dysfunction associated with a putative late-onset phenotype. Rheobase, threshold potential, and resting membrane potential as key parameters reflecting membrane excitability [18,41,46] were not different compared to controls (Fig. 4). Interestingly, we found a reduced AP firing frequency for S126G neurons when stimulated with 2× rheobase current, while no difference was observed for both lower and higher suprathreshold currents. In a study on gain-of-function variants of the voltage-gated sodium channel $Na_v1.8$, increase rather than decrease in firing frequency was directly linked to neuropathic pain [22]. Therefore, mere reduction of AP firing frequency without apparent influence on other AP parameters and only in one of the tested stimulus conditions is considered a finding without biological relevance. Together with the unremarkable neurological examination, our results add further evidence that determination of IENFD alone is not sufficient for diagnosing small fiber neuropathy and associated FD.

An intrinsic limitation of our study is the focus on one individual carrying the S126G variant. As reported before, phenotypic diversity

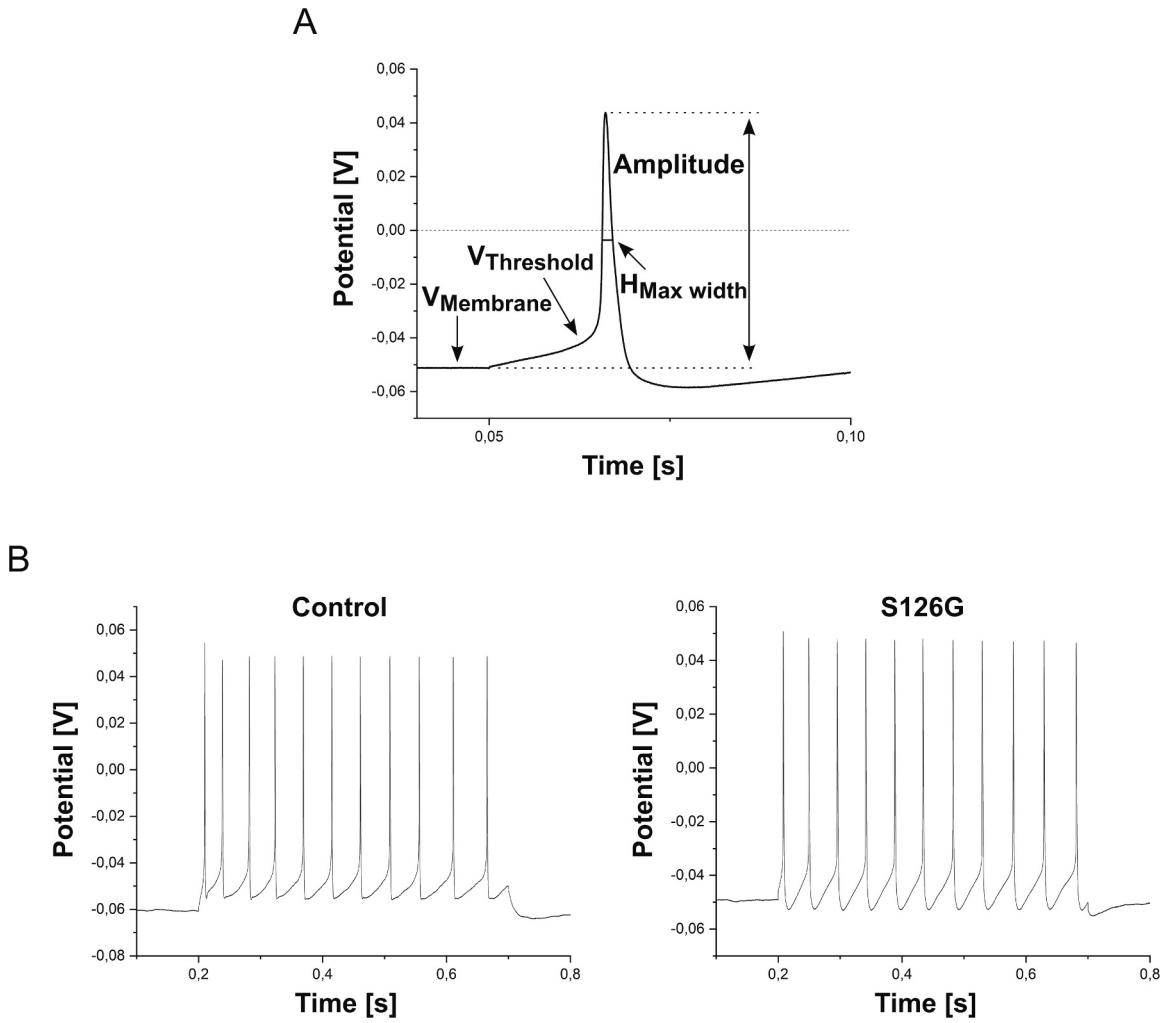

Fig. 3. Depiction of AP parameters and repetitive firing.
(A) Representative AP recorded from a S126G sensory neuron. Resting membrane potential ($V_{Membrane}$), threshold potential ($V_{Threshold}$), AP duration ($H_{Max\ width}$), and amplitude are indicated. (B) Representative current clamp recordings of repetitive AP firing in control and S126 sensory neurons. AP trains were elicited by 500 ms current injection equivalent to 2× rheobase current. Abbreviations: AP, action potential.

occurs in patients sharing the same *GLA* variant [9]. In women, this might be ascribed to random X-inactivation and subsequent difference in cell-to-cell enzyme activity [45,73]. Since severe phenotypic variability was also found in men and even within one family [55], epigenetic modifications were proposed as an explanation [75]. However, phenotypic variability is mainly reported for variants abolishing α-GAL A activity [9,55,75], hence reflecting resilience to enzyme malfunction. Patient-to-patient variability is therefore expected to be a minor issue with variants allowing for normal enzyme activity.

We present translational data combining clinical examination and *in vitro* research to assess the effect of the VUS S126G in FD-associated *GLA* gene. Our findings suggest no pathological effects of this variant on enzyme activity and overall cellular fate and add to the evidence categorizing the S126G as benign.

Author contributions

Maximilian Breyer: Methodology, Formal analysis, Investigation, Writing – Original Draft, Visualization. **Julia Grüner:** Methodology, Investigation. **Alexandra Klein:** Methodology, Formal analysis, Investigation. **Laura Finke:** Investigation. **Katharina Klug:** Methodology. **Markus Sauer:** Project administration, Funding acquisition. **Nurcan Üçeyler:** Conceptualization, Resources, Writing – Original Draft, Supervision, Project administration, Funding acquisition.

Funding

This project was supported by the Interdisciplinary Center for Clinical Research Würzburg (Interdisziplinäres Zentrum für Klinische Forschung (IZKF); N-375) and by the German Research Foundation (Deutsche Forschungsgemeinschaft (DFG), Sonderforschungsbereich SFB1158). J.G. was supported by DFG (KFO5001 ResolvePAIN, project ID: 426503586). N.Ü. was supported by DFG (UE171/15-1).

Institutional review board statement

The study was approved by the Ethics Committee of the University of Würzburg Medical Faculty (#26/19) on 11 September 2019.

Informed consent statement

Informed consent was obtained from all subjects involved in the study. Written informed consent has been obtained from the patient to publish this paper.

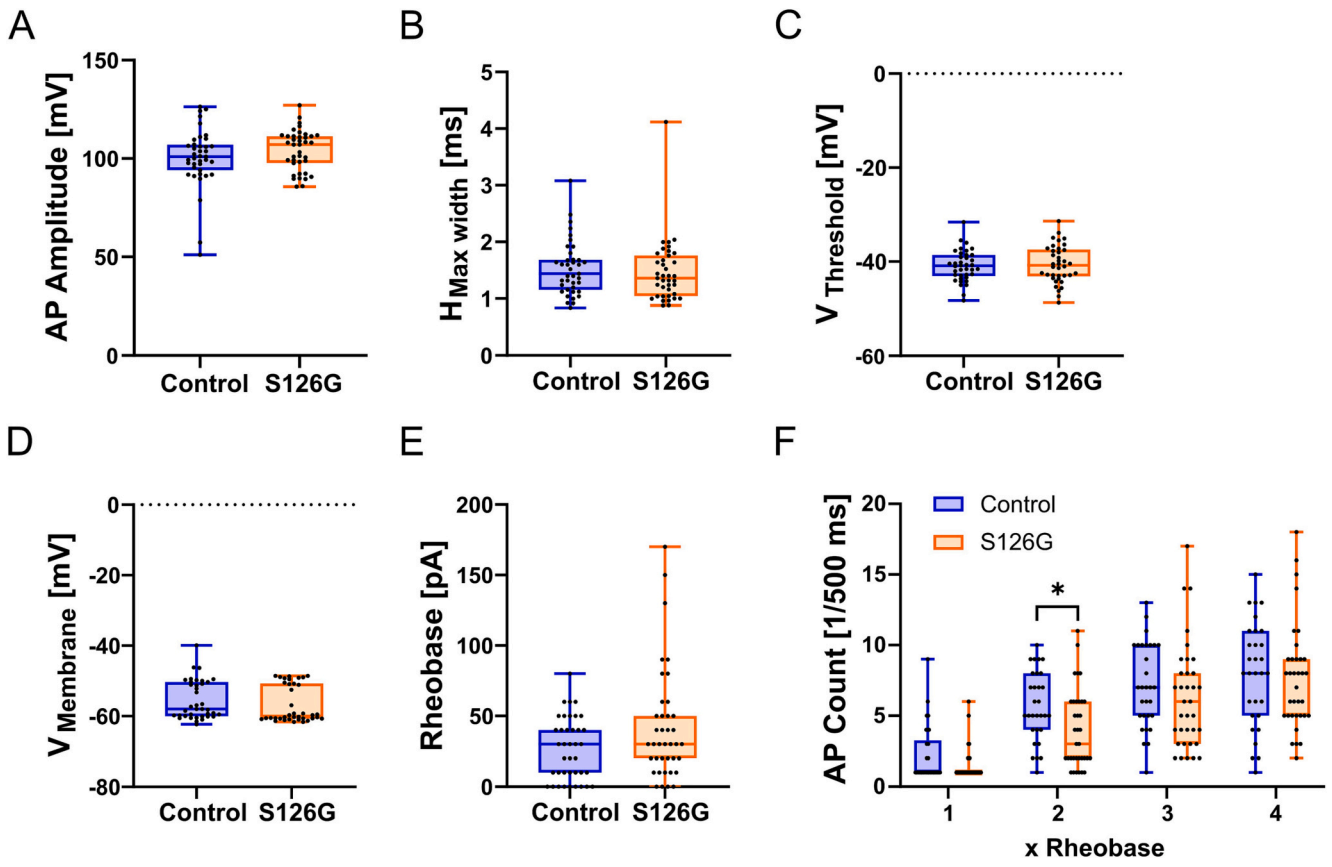

Fig. 4. Analysis of AP characteristics, membrane potential, and firing frequency in S126G and healthy control sensory neurons.
(A) AP amplitude ($n_{Control} = 39$, $n_{S126G} = 39$), (B) AP duration ($H_{Max\ width}$, $n_{Control} = 39$, $n_{S126G} = 39$), (C) threshold potential ($V_{Threshold}$, $n_{Control} = 38$, $n_{S126G} = 38$), and (D) resting membrane potential ($V_{Membrane}$, $n_{Control} = 38$, $n_{S126G} = 38$) showed no differences between S126G and healthy control neurons. (E) The minimum current to elicit an AP (Rheobase, $n_{Control} = 39$, $n_{S126G} = 39$) showed no difference between S126G neurons and healthy control neurons. (F) Neuronal firing frequency determined by AP counts within 500 ms of stimulation with multiples of the rheobase showed no difference between S126G and healthy control neurons for 1×, 3×, and 4× rheobase ($n_{Control} = 30$, $n_{S126G} = 35$), while firing frequency was reduced in S126G neurons for 2× rheobase ($p < 0.05$). Data was collected and pooled from two clones per iPSC line and a minimum of three independent differentiations. *$p < 0.05$. Box and whisker plots with min to max and single data points. Abbreviations: AP, action potential.

CRediT authorship contribution statement

Maximilian Breyer: Conceptualization, Formal analysis, Investigation, Methodology, Validation, Visualization, Writing – original draft. **Julia Grüner:** Formal analysis, Methodology, Validation, Writing – review & editing. **Alexandra Klein:** Formal analysis, Methodology, Writing – review & editing. **Laura Finke:** Formal analysis, Methodology, Writing – review & editing. **Katharina Klug:** Formal analysis, Methodology, Writing – review & editing. **Markus Sauer:** Conceptualization, Funding acquisition, Supervision, Writing – review & editing. **Nurcan Üçeyler:** Conceptualization, Funding acquisition, Project administration, Resources, Supervision, Writing – original draft.

Author statement

Data is available upon request from the corresponding author.

Declaration of Competing Interest

The authors declare no conflict of interest. The funders had no role in the design of the study; in the collection, analyses, or interpretation of data; in the writing of the manuscript, or in the decision to publish the results.

Data availability

Data will be made available on request.

Acknowledgments

We thank Daniela Urlaub and Danilo Prtvar, M.Sc. (Department of Neurology, University of Würzburg, 97080 Würzburg, Germany) for excellent technical assistance. We further thank Dr. Jan Schlegel (Department of Biophysics and Biotechnology, Biocenter, University of Würzburg, 97074 Würzburg, Germany) for help with fluorescent Shiga toxin coupling. We also thank Dr. Thomas Klein (Department of Neurology, University of Würzburg, 97080 Würzburg, Germany) for the establishment of iPSC-based sensory neuron generation in our group. We further thank Prof. Dr. Eva Klopocki (Institute for Human Genetics, University of Würzburg, 97074 Würzburg, Germany) for karyotype analysis of iPSC clones.

Appendix A. Supplementary data

Supplementary data to this article can be found online at https://doi.org/10.1016/j.ymgmr.2023.101029.

References

[1] M.A. Alhazzaa, A. Mujtaba, M.A. Aljohani, F. Alqarni, R. Alsharif, The prevalence of Fabry disease among young cryptogenic stroke patients, Cureus 12 (7) (2020), e9415, https://doi.org/10.7759/cureus.9415.

[2] G.M. Altarescu, L.G. Goldfarb, K.Y. Park, C. Kaneski, N. Jeffries, S. Litvak, J. W. Nagle, R. Schiffmann, Identification of fifteen novel mutations and genotype-phenotype relationship in Fabry disease, Clin. Genet. 60 (1) (2001) 46–51, https://doi.org/10.1034/j.1399-0004.2001.600107.x.

[3] M. Arends, C. Wanner, D. Hughes, A. Mehta, D. Oder, O.T. Watkinson, P.M. Elliott, G.E. Linthorst, F.A. Wijburg, M. Biegstraaten, C.E. Hollak, Characterization of classical and nonclassical Fabry disease: A multicenter study, J. Am. Soc. Nephrol. 28 (5) (2017) 1631–1641, https://doi.org/10.1681/ASN.2016090964.

[4] O. Aydin, C.S. Kasapkara, G.E. Celik, Successful desensitization with agalsidase alfa in 2 brothers with Fabry disease, J Investig Allergol Clin Immunol 23 (5) (2013) 367–368. http://www.ncbi.nlm.nih.gov/pubmed/24260986.

[5] F. Barbey, F. Livio, Safety of enzyme replacement therapy, in: A. Mehta, M. Beck, G. Sunder-Plassmann (Eds.), Fabry Disease: Perspectives from 5 Years of FOS, Oxford, 2006. http://www.ncbi.nlm.nih.gov/pubmed/21290709.

[6] E.R. Benjamin, M.C. Della Valle, X. Wu, E. Katz, F. Pruthi, S. Bond, B. Bronfin, H. Williams, J. Yu, D.G. Bichet, D.P. Germain, R. Giugliani, D. Hughes, R. Schiffmann, W.R. Wilcox, R.J. Desnick, J. Kirk, J. Barth, C. Barlow, K. J. Valenzano, J. Castelli, D.J. Lockhart, The validation of pharmacogenetics for the identification of Fabry patients to be treated with migalastat, Genet. Med. 19 (4) (2017) 430–438, https://doi.org/10.1038/gim.2016.122.

[7] G. Biagini, A. Almeida, T.V.R. Almeida, C.A.B. Silva, B.F. Castro, T.C. Reche, A. C. Dabinski, F.C. Barreto, Case report: is low alpha-Gal enzyme activity sufficient to establish the diagnosis of Fabry disease? J. Bras. Nefrol. 39 (3) (2017) 333–336, https://doi.org/10.5935/0101-2800.20170057.

[8] M. Breyer, T. Klein, K. Klug, E. Klopocki, N. Üçeyler, Generation of the induced pluripotent stem cell line UKWNLi005-A derived from a patient with the GLA mutation c.376A > G of unknown pathogenicity in Fabry disease, Stem Cell Res. 61 (2022), 102747, https://doi.org/10.1016/j.scr.2022.102747.

[9] G. Cammarata, P. Fatuzzo, M.S. Rodolico, P. Colomba, L. Sicurella, F. Iemolo, C. Zizzo, R. Alessandro, C. Bartolotta, G. Duro, I. Monte, High variability of Fabry disease manifestations in an extended Italian family, Biomed. Res. Int. 2015 (2015), 504784, https://doi.org/10.1155/2015/504784.

[10] A.B. Celi, J. Goldstein, M.V. Rosato-Siri, A. Pinto, Role of Globotriaosylceramide in physiology and pathology, Front. Mol. Biosci. 9 (2022), 813637, https://doi.org/10.3389/fmolb.2022.813637.

[11] S. Chen, L.C. Francioli, J.K. Goodrich, R.L. Collins, M. Kanai, Q. Wang, J. Alföldi, N. A. Watts, C. Vittal, L.D. Gauthier, T. Poterba, M.W. Wilson, Y. Tarasova, W. Phu, M. T. Yohannes, Z. Koenig, Y. Farjoun, E. Banks, S. Donnelly, S. Gabriel, N. Gupta, S. Ferriera, C. Tolonen, S. Novod, L. Bergelson, D. Roazen, V. Ruano-Rubio, M. Covarrubias, C. Llanwarne, N. Petrillo, G. Wade, T. Jeandet, R. Munshi, K. Tibbetts, G.P. Consortium, A. O'Donnell-Luria, M. Solomonson, C. Seed, A. R. Martin, M.E. Talkowski, H.L. Rehm, M.J. Daly, G. Tiao, B.M. Neale, D. G. MacArthur, K.J. Karczewski, A genome-wide mutational constraint map quantified from variation in 76,156 human genomes, bioRxiv (2022), https://doi.org/10.1101/2022.03.20.485034, 2022.2003.2020.485034.

[12] M. Connock, A. Juarez-Garcia, E. Frew, A. Mans, J. Dretzke, A. Fry-Smith, D. Moore, A systematic review of the clinical effectiveness and cost-effectiveness of enzyme replacement therapies for Fabry's disease and mucopolysaccharidosis type 1, Health Technol. Assess. 10 (20) (2006), https://doi.org/10.3310/hta10200 iii-iv, ix-113.

[13] A. Corry, C. Feighery, D. Alderdice, F. Stewart, M. Walsh, O.M. Dolan, A family with Fabry disease diagnosed by a single angiokeratoma, Dermatol. Online J. 17 (4) (2011) 5. http://www.ncbi.nlm.nih.gov/pubmed/21549080.

[14] S. Davidson, B.A. Copits, J. Zhang, G. Page, A. Ghetti, R.W. Gereau 4th, Human sensory neurons: membrane properties and sensitization by inflammatory mediators, Pain 155 (9) (2014) 1861–1870, https://doi.org/10.1016/j.pain.2014.06.017.

[15] I. De Brabander, L. Yperzeele, C. Ceuterick-De Groote, R. Brouns, R. Baker, S. Belachew, J. Delbecq, G. De Keulenaer, S. Dethy, F. Eyskens, A. Fumal, D. Hemelsoet, D. Hughes, S. Jeangette, D. Nuytten, P. Redondo, B. Sadzot, C. Sindic, R. Sheorajpanday, V. Thijs, C. Van Broeckhoven, P.P. De Deyn, Phenotypical characterization of alpha-galactosidase A gene mutations identified in a large Fabry disease screening program in stroke in the young, Clin. Neurol. Neurosurg. 115 (7) (2013) 1088–1093, https://doi.org/10.1016/j.clineuro.2012.11.003.

[16] M. du Moulin, A.F. Koehn, A. Golsari, S. Dulz, Y. Atiskova, M. Patten, J. Münch, M. Avanesov, K. Ullrich, N. Muschol, The mutation p.D313Y is associated with organ manifestation in Fabry disease, Clin. Genet. 92 (5) (2017) 528–533, https://doi.org/10.1111/cge.13007.

[17] V. Dubuc, D.F. Moore, L.C. Gioia, G. Saposnik, D. Selchen, S. Lanthier, Prevalence of Fabry disease in young patients with cryptogenic ischemic stroke, J. Stroke Cerebrovasc. Dis. 22 (8) (2013) 1288–1292, https://doi.org/10.1016/j.jstrokecerebrovasdis.2012.10.005.

[18] D.E. Duzhyy, N.V. Voitenko, P.V. Belan, Peripheral inflammation results in increased excitability of capsaicin-insensitive nociceptive DRG neurons mediated by upregulation of ASICs and voltage-gated ion channels, Front. Cell. Neurosci. 15 (2021), 723295, https://doi.org/10.3389/fncel.2021.723295.

[19] N. Egenolf, C.M. Zu Altenschildesche, L. Kreß, K. Eggermann, B. Namer, F. Gross, A. Klitsch, T. Malzacher, D. Kampik, R.A. Malik, I. Kurth, C. Sommer, N. Üçeyler, Diagnosing small fiber neuropathy in clinical practice: a deep phenotyping study, Ther. Adv. Neurol. Disord. 14 (2021), https://doi.org/10.1177/17562864211004318, 17562864211004318.

[20] R. El-Abassi, D. Singhal, J.D. England, Fabry's disease, J. Neurol. Sci. 344 (1–2) (2014) 5–19, https://doi.org/10.1016/j.jns.2014.06.029.

[21] C.M. Eng, J. Fletcher, W.R. Wilcox, S. Waldek, C.R. Scott, D.O. Sillence, F. Breunig, J. Charrow, D.P. Germain, K. Nicholls, M. Banikazemi, Fabry disease: baseline medical characteristics of a cohort of 1765 males and females in the Fabry registry, J. Inherit. Metab. Dis. 30 (2) (2007) 184–192, https://doi.org/10.1007/s10545-007-0521-2.

[22] C.G. Faber, G. Lauria, I.S. Merkies, X. Cheng, C. Han, H.S. Ahn, A.K. Persson, J. G. Hoeijmakers, M.M. Gerrits, T. Pierro, R. Lombardi, D. Kapetis, S.D. Dib-Hajj, S. G. Waxman, Gain-of-function Nav1.8 mutations in painful neuropathy, Proc. Natl. Acad. Sci. U. S. A. 109 (47) (2012) 19444–19449, https://doi.org/10.1073/pnas.1216080109.

[23] S.C. Garman, D.N. Garboczi, Structural basis of Fabry disease, Mol. Genet. Metab. 77 (1–2) (2002) 3–11, https://doi.org/10.1016/s1096-7192(02)00151-8.

[24] S.C. Garman, D.N. Garboczi, The molecular defect leading to Fabry disease: structure of human alpha-galactosidase, J. Mol. Biol. 337 (2) (2004) 319–335, https://doi.org/10.1016/j.jmb.2004.01.035.

[25] D.P. Germain, Fabry disease, Orphanet J. Rare Dis. 5 (2010) 30, https://doi.org/10.1186/1750-1172-5-30.

[26] D.P. Germain, P.M. Elliott, B. Falissard, V.V. Fomin, M.J. Hilz, A. Jovanovic, I. Kantola, A. Linhart, R. Mignani, M. Namdar, A. Nowak, J.P. Oliveira, M. Pieroni, M. Viana-Baptista, C. Wanner, M. Spada, The effect of enzyme replacement therapy on clinical outcomes in male patients with Fabry disease: A systematic literature review by a European panel of experts, Mol. Genet. Metab. Rep. 19 (2019), 100454, https://doi.org/10.1016/j.ymgmr.2019.100454.

[27] D.P. Germain, T. Levade, E. Hachulla, B. Knebelmann, D. Lacombe, V.L. Seguin, K. Nguyen, E. Noël, J.P. Rabès, Challenging the traditional approach for interpreting genetic variants: lessons from Fabry disease, Clin. Genet. 101 (4) (2022) 390–402, https://doi.org/10.1111/cge.14102.

[28] J.F. Guest, D. Concolino, R. Di Vito, C. Feliciani, R. Parini, A. Zampetti, Modelling the resource implications of managing adults with Fabry disease in Italy, Eur. J. Clin. Investig. 41 (7) (2011) 710–718, https://doi.org/10.1111/j.1365-2362.2010.02458.x.

[29] S.J. Guzman, A. Schlögl, C. Schmidt-Hieber, Stimfit: quantifying electrophysiological data with Python, Front. Neuroinform. 8 (2014) 16, https://doi.org/10.3389/fninf.2014.00016.

[30] L. Hasholt, M. Ballegaard, H. Bundgaard, M. Christiansen, I. Law, A.M. Lund, A. Norremolle, A. Krogh Rasmussen, K. Ravn, Z. Tumer, F. Wibrand, U. Feldt-Rasmussen, The D313Y variant in the GLA gene - no evidence of a pathogenic role in Fabry disease, Scand. J. Clin. Lab. Invest. 77 (8) (2017) 617–621, https://doi.org/10.1080/00365513.2017.1390782.

[31] B. Hoffmann, H. Georg Koch, S. Schweitzer-Krantz, U. Wendel, E. Mayatepek, Deficient alpha-galactosidase A activity in plasma but no Fabry disease–a pitfall in diagnosis, Clin. Chem. Lab. Med. 43 (11) (2005) 1276–1277, https://doi.org/10.1515/CCLM.2005.219.

[32] S.C. Jung, I.P. Han, A. Limaye, R. Xu, M.P. Gelderman, P. Zerfas, K. Tirumalai, G. J. Murray, M.J. During, R.O. Brady, P. Qasba, Adeno-associated viral vector-mediated gene transfer results in long-term enzymatic and functional correction in multiple organs of Fabry mice, Proc. Natl. Acad. Sci. U. S. A. 98 (5) (2001) 2676–2681, https://doi.org/10.1073/pnas.051634498.

[33] C.R. Kaneski, J.A. Hanover, U.H. Schueler Hoffman, Generation of GLA-knockout human embryonic stem cell lines to model peripheral neuropathy in Fabry disease, Mol. Genet. Metab. Rep. 33 (2022), 100914, https://doi.org/10.1016/j.ymgmr.2022.100914.

[34] F. Karl, M. Wußmann, L. Kreß, T. Malzacher, P. Fey, F. Groeber-Becker, N. Üçeyler, Patient-derived in vitro skin models for investigation of small fiber pathology, Ann. Clin. Transl. Neurol. 6 (9) (2019) 1797–1806, https://doi.org/10.1002/acn3.50871.

[35] M.A. Kelley, K.V. Hackshaw, Intraepidermal nerve Fiber density as measured by skin punch biopsy as a marker for small Fiber neuropathy: application in patients with fibromyalgia, Diagnostics (Basel) 11 (3) (2021), https://doi.org/10.3390/diagnostics11030536.

[36] T. Klein, J. Grüner, M. Breyer, J. Schlegel, N.M. Schottmann, L. Hofmann, K. Gauss, R. Mease, C. Erbacher, L. Finke, A. Klein, K. Klug, F. Karl-Schöller, B. Vignolo, S. Reinhard, T. Schneider, K. Günther, J. Fink, J. Dudek, C. Maack, E. Klopocki, J. Seibel, F. Edenhofer, E. Wischmeyer, M. Sauer, N. Üçeyler, Small fibre neuropathy in Fabry disease: a human-derived neuronal *in vitro* disease model, bioRxiv (2023), https://doi.org/10.1101/2023.08.09.552621, 2023.2008.2009.552621.

[37] M.J. Landrum, J.M. Lee, M. Benson, G.R. Brown, C. Chao, S. Chitipiralla, B. Gu, J. Hart, D. Hoffman, W. Jang, K. Karapetyan, K. Katz, C. Liu, Z. Maddipatla, A. Malheiro, K. McDaniel, M. Ovetsky, G. Riley, G. Zhou, J.B. Holmes, B. L. Kattman, D.R. Maglott, ClinVar: improving access to variant interpretations and supporting evidence, Nucleic Acids Res. 46 (D1) (2018) D1062–D1067, https://doi.org/10.1093/nar/gkx1153.

[38] S. Lanthier, G. Saposnik, G. Lebovic, K. Pope, D. Selchen, D.F. Moore, Canadian Fabry Stroke Screening Initiative Study, G, Prevalence of Fabry disease and outcomes in young Canadian patients with cryptogenic ischemic cerebrovascular events, Stroke 48 (7) (2017) 1766–1772, https://doi.org/10.1161/STROKEAHA.116.016083.

[39] K. Lau, N. Üçeyler, T. Cairns, L. Lorenz, C. Sommer, M. Schindehütte, K. Amann, C. Wanner, P. Nordbeck, Gene variants of unknown significance in Fabry disease: clinical characteristics of c.376A>G (p.Ser126Gly), Mol. Genet. Genomic Med. 10 (5) (2022), e1912, https://doi.org/10.1002/mgg3.1912.

[40] G. Lauria, S.T. Hsieh, O. Johansson, W.R. Kennedy, J.M. Leger, S.I. Mellgren, M. Nolano, I.S. Merkies, M. Polydefkis, A.G. Smith, C. Sommer, J. Valls-Solé, European Federation of Neurological, S., Peripheral Nerve, S, European Federation of Neurological Societies/Peripheral Nerve Society Guideline on the use of skin biopsy in the diagnosis of small fiber neuropathy. Report of a joint task force of the European Federation of Neurological Societies and the Peripheral Nerve Society, Eur. J. Neurol. 17 (7) (2010) 903–912, e944-909, https://doi.org/10.1111/j.1468-1331.2010.03023.x.

[41] B. Liu, H. Li, S.J. Brull, J.M. Zhang, Increased sensitivity of sensory neurons to tumor necrosis factor alpha in rats with chronic compression of the lumbar ganglia, J. Neurophysiol. 88 (3) (2002) 1393–1399, https://doi.org/10.1152/jn.2002.88.3.1393.

[42] J. Lukas, A.K. Giese, A. Markoff, U. Grittner, E. Kolodny, H. Mascher, K.J. Lackner, W. Meyer, P. Wree, V. Saviouk, A. Rolfs, Functional characterisation of alpha-galactosidase a mutations as a basis for a new classification system in fabry disease, PLoS Genet. 9 (8) (2013), e1003632, https://doi.org/10.1371/journal.pgen.1003632.

[43] W. Magerl, E.K. Krumova, R. Baron, T. Tölle, R.D. Treede, C. Maier, Reference data for quantitative sensory testing (QST): refined stratification for age and a novel method for statistical comparison of group data, Pain 151 (3) (2010) 598–605, https://doi.org/10.1016/j.pain.2010.07.026.

[44] I. Majoul, T. Schmidt, M. Pomasanova, E. Boutkevich, Y. Kozlov, H.D. Söling, Differential expression of receptors for Shiga and cholera toxin is regulated by the cell cycle, J. Cell Sci. 115 (Pt 4) (2002) 817–826, https://doi.org/10.1242/jcs.115.4.817.

[45] A. Mehta, R. Ricci, U. Widmer, F. Dehout, A. Garcia de Lorenzo, C. Kampmann, A. Linhart, G. Sunder-Plassmann, M. Ries, M. Beck, Fabry disease defined: baseline clinical manifestations of 366 patients in the Fabry outcome survey, Eur. J. Clin. Investig. 34 (3) (2004) 236–242, https://doi.org/10.1111/j.1365-2362.2004.01309.x.

[46] B. Namer, K. Ørstavik, R. Schmidt, N. Mair, I.P. Kleggetveit, M. Zeidler, T. Martha, E. Jorum, M. Schmelz, T. Kalpachidou, M. Kress, M. Langeslag, Changes in ionic conductance signature of nociceptive neurons underlying Fabry disease phenotype, Front. Neurol. 8 (2017) 335, https://doi.org/10.3389/fneur.2017.00335.

[47] K. Nicholls, K. Bleasel, G. Becker, Severe infusion reactions to fabry enzyme replacement therapy: rechallenge after tracheostomy, JIMD Rep. 5 (2012) 109–112, https://doi.org/10.1007/8904_2011_106.

[48] M. Niemann, A. Rolfs, A. Giese, H. Mascher, F. Breunig, G. Ertl, C. Wanner, F. Weidemann, Lyso-Gb3 indicates that the alpha-galactosidase A mutation D313Y is not clinically relevant for Fabry disease, JIMD Rep. 7 (2013) 99–102, https://doi.org/10.1007/8904_2012_154.

[49] S. Oommen, Y. Zhou, M. Meiyappan, A. Gurevich, Y. Qiu, Inter-assay variability influences migalastat amenability assessments among Fabry disease variants, Mol. Genet. Metab. 127 (1) (2019) 74–85, https://doi.org/10.1016/j.ymgme.2019.04.005.

[50] R. Ornello, D. Degan, C. Tiseo, C. Di Carmine, L. Perciballi, F. Pistoia, A. Carolei, S. Sacco, Distribution and temporal trends from 1993 to 2015 of ischemic stroke subtypes: A systematic review and Meta-analysis, Stroke 49 (4) (2018) 814–819, https://doi.org/10.1161/STROKEAHA.117.020031.

[51] R.C. Reisin, J. Mazziotti, L.L. Cejas, A. Zinnerman, P. Bonardo, M.F. Pardal, A. Martinez, P. Riccio, S. Ameriso, E. Bendersky, P. Nofal, P. Cairola, L. Jure, A. Sotelo, P. Rozenfeld, R. Ceci, I. Casas-Parera, A. Sanchez-Luceros, A. Investigators, Prevalence of Fabry disease in young patients with stroke in Argentina, J. Stroke Cerebrovasc. Dis. 27 (3) (2018) 575–582, https://doi.org/10.1016/j.jstrokecerebrovasdis.2017.09.045.

[52] S. Richards, N. Aziz, S. Bale, D. Bick, S. Das, J. Gastier-Foster, W.W. Grody, M. Hegde, E. Lyon, E. Spector, K. Voelkerding, H.L. Rehm, A.L.Q.A. Committee, Standards and guidelines for the interpretation of sequence variants: a joint consensus recommendation of the American College of Medical Genetics and Genomics and the Association for Molecular Pathology, Genet. Med. 17 (5) (2015) 405–424, https://doi.org/10.1038/gim.2015.30.

[53] V. Rickert, L. Wagenhäuser, P. Nordbeck, C. Wanner, C. Sommer, S. Rost, N. Üçeyler, Stratification of Fabry mutations in clinical practice: a closer look at alpha-galactosidase A-3D structure, J. Intern. Med. 288 (5) (2020) 593–604, https://doi.org/10.1111/joim.13125.

[54] C. Riera, S. Lois, C. Domínguez, I. Fernandez-Cadenas, J. Montaner, V. Rodríguez-Sureda, X. de la Cruz, Molecular damage in Fabry disease: characterization and prediction of alpha-galactosidase A pathological mutations, Proteins 83 (1) (2015) 91–104, https://doi.org/10.1002/prot.24708.

[55] M. Rigoldi, D. Concolino, A. Morrone, F. Pieruzzi, R. Ravaglia, F. Furlan, F. Santus, P. Strisciuglio, G. Torti, R. Parini, Intrafamilial phenotypic variability in four families with Anderson-Fabry disease, Clin. Genet. 86 (3) (2014) 258–263, https://doi.org/10.1111/cge.12261.

[56] C. Riillo, G. Bonapace, M.T. Moricca, S. Sestito, A. Salatino, D. Concolino, c.376A>G, (p.Ser126Gly) Alpha-Galactosidase A mutation induces ER stress, unfolded protein response and reduced enzyme trafficking to lysosome: Possible relevance in the pathogenesis of late-onset forms of Fabry Disease, Mol. Genet. Metab. 140 (3) (2023) 107700, https://doi.org/10.1016/j.ymgme.2023.107700.

[57] A. Sagnelli, M. Savoiardo, C. Marchesi, L. Morandi, M. Mora, M. Morbin, L. Farina, A. Mazzeo, A. Toscano, S. Pagliarani, S. Lucchiari, G.P. Comi, E. Salsano, D. Pareyson, Adult polyglucosan body disease in a patient originally diagnosed with Fabry's disease, Neuromuscul. Disord. 24 (3) (2014) 272–276, https://doi.org/10.1016/j.nmd.2013.11.006.

[58] H. Sarikaya, M. Yilmaz, N. Michael, A.R. Miserez, B. Steinmann, R. W. Baumgartner, Zurich Fabry study - prevalence of Fabry disease in young patients with first cryptogenic ischaemic stroke or TIA, Eur. J. Neurol. 19 (11) (2012) 1421–1426, https://doi.org/10.1111/j.1468-1331.2012.03737.x.

[59] R. Schiffmann, M. Fuller, L.A. Clarke, J.M. Aerts, Is it Fabry disease? Genet. Med. 18 (12) (2016) 1181–1185, https://doi.org/10.1038/gim.2016.55.

[60] J. Schindelin, I. Arganda-Carreras, E. Frise, V. Kaynig, M. Longair, T. Pietzsch, S. Preibisch, C. Rueden, S. Saalfeld, B. Schmid, J.Y. Tinevez, D.J. White, V. Hartenstein, K. Eliceiri, P. Tomancak, A. Cardona, Fiji: an open-source platform for biological-image analysis, Nat. Methods 9 (7) (2012) 676–682, https://doi.org/10.1038/nmeth.2019.

[61] J. Schlegel, M. Sauer, Superresolution microscopy of sphingolipids, Methods Mol. Biol. 2187 (2021) 303–311, https://doi.org/10.1007/978-1-0716-0814-2_17.

[62] S.H. Shin, S. Kluepfel-Stahl, A.M. Cooney, C.R. Kaneski, J.M. Quirk, R. Schiffmann, R.O. Brady, G.J. Murray, Prediction of response of mutated alpha-galactosidase A to a pharmacological chaperone, Pharmacogenet. Genomics 18 (9) (2008) 773–780, https://doi.org/10.1097/FPC.0b013e32830500f4.

[63] B.E. Smid, S.L. Hoogendijk, F.A. Wijburg, C.E. Hollak, G.E. Linthorst, A revised home treatment algorithm for Fabry disease: influence of antibody formation, Mol. Genet. Metab. 108 (2) (2013) 132–137, https://doi.org/10.1016/j.ymgme.2012.12.005.

[64] B.E. Smid, C.E. Hollak, B.J. Poorthuis, M.A. van den Bergh Weerman, S. Florquin, W.E. Kok, R.H. Lekanne Deprez, J. Timmermans, G.E. Linthorst, Diagnostic dilemmas in Fabry disease: a case series study on GLA mutations of unknown clinical significance, Clin. Genet. 88 (2) (2015) 161–166, https://doi.org/10.1111/cge.12449.

[65] A.G. Smith, J.R. Howard, R. Kroll, P. Ramachandran, P. Hauer, J.R. Singleton, J. McArthur, The reliability of skin biopsy with measurement of intraepidermal nerve fiber density, J. Neurol. Sci. 228 (1) (2005) 65–69, https://doi.org/10.1016/j.jns.2004.09.032.

[66] P.D. Stenson, M. Mort, E.V. Ball, M. Chapman, K. Evans, L. Azevedo, M. Hayden, S. Heywood, D.S. Millar, A.D. Phillips, D.N. Cooper, The human gene mutation database (HGMD((R))): optimizing its use in a clinical diagnostic or research setting, Hum. Genet. 139 (10) (2020) 1197–1207, https://doi.org/10.1007/s00439-020-02199-3.

[67] C. Tesmoingt, O. Lidove, A. Reberga, M. Thetis, C. Ackaert, P. Nicaise, P. Arnaud, T. Papo, Enzyme therapy in Fabry disease: severe adverse events associated with anti-agalsidase cross-reactive IgG antibodies, Br. J. Clin. Pharmacol. 68 (5) (2009) 765–769, https://doi.org/10.1111/j.1365-2125.2009.03501.x.

[68] N. Üçeyler, W. Kafke, N. Riediger, L. He, G. Necula, K.V. Toyka, C. Sommer, Elevated proinflammatory cytokine expression in affected skin in small fiber neuropathy, Neurology 74 (22) (2010) 1806–1813, https://doi.org/10.1212/WNL.0b013e3181e0f7b3.

[69] N. Üçeyler, S. Ganendiran, D. Kramer, C. Sommer, Characterization of pain in fabry disease, Clin. J. Pain 30 (10) (2014) 915–920, https://doi.org/10.1097/AJP.0000000000000041.

[70] K. Valtola, J. Nino-Quintero, M. Hedman, L. Lottonen-Raikaslehto, T. Laitinen, M. Maria, I. Kantola, A. Naukkarinen, M. Laakso, J. Kuusisto, Cardiomyopathy associated with the Ala143Thr variant of the alpha-galactosidase A gene, Heart 106 (8) (2020) 609–615, https://doi.org/10.1136/heartjnl-2019-315933.

[71] L. van der Tol, C. Verhamme, I.N. van Schaik, A.J. van der Kooi, C.E. Hollak, M. Biegstraaten, In patients with an alpha-galactosidase A variant, small nerve fibre assessment cannot confirm a diagnosis of Fabry disease, JIMD Rep. 28 (2016) 95–103, https://doi.org/10.1007/8904_2015_503.

[72] M. Veroux, I.P. Monte, M.S. Rodolico, D. Corona, R. Bella, A. Basile, S. Palmucci, M.L. Pistorio, G. Lanza, C. De Pasquale, P. Veroux, Screening for Fabry disease in kidney transplant recipients: experience of a multidisciplinary team, Biomedicines 8 (10) (2020), https://doi.org/10.3390/biomedicines8100396.

[73] L. Wagenhäuser, V. Rickert, C. Sommer, C. Wanner, P. Nordbeck, S. Rost, N. Üçeyler, X-chromosomal inactivation patterns in women with Fabry disease, Mol. Genet. Genomic Med. 10 (9) (2022), e2029, https://doi.org/10.1002/mgg3.2029.

[74] F. Weidemann, A. Jovanovic, K. Herrmann, I. Vardarli, Chaperone therapy in Fabry disease, Int. J. Mol. Sci. 23 (3) (2022), https://doi.org/10.3390/ijms23031887.

[75] S. Yamamoto, T. Nagasawa, K. Sugimura, A. Kanno, S. Tatebe, T. Aoki, H. Sato, K. Kozu, R. Konno, K. Nochioka, K. Satoh, H. Shimokawa, Clinical diversity in patients with Anderson-fabry disease with the R301Q mutation, Intern. Med. 58 (4) (2019) 603–607, https://doi.org/10.2169/internalmedicine.0959-18.

[76] C. Zompola, L. Palaiodimou, P. Kokotis, M. Papadopoulou, A. Theodorou, N. Sabanis, E. Theodoroula, M. Papathanasiou, G. Tsivgoulis, E. Chroni, The mutation D313Y may be associated with nervous system manifestations in Fabry disease, J. Neurol. Sci. 412 (2020), 116757, https://doi.org/10.1016/j.jns.2020.116757.